JAAS

Accepted Manuscript

This is an *Accepted Manuscript*, which has been through the Royal Society of Chemistry peer review process and has been accepted for publication.

Accepted Manuscripts are published online shortly after acceptance, before technical editing, formatting and proof reading. Using this free service, authors can make their results available to the community, in citable form, before we publish the edited article. We will replace this *Accepted Manuscript* with the edited and formatted *Advance Article* as soon as it is available.

You can find more information about *Accepted Manuscripts* in the Information for Authors.

Please note that technical editing may introduce minor changes to the text and/or graphics, which may alter content. The journal's standard Terms & Conditions and the Ethical guidelines still apply. In no event shall the Royal Society of Chemistry be held responsible for any errors or omissions in this *Accepted Manuscript* or any consequences arising from the use of any information it contains.

ROYAL SOCIETY OF CHEMISTRY

www.rsc.org/jaas

Elemental recoveries for metal oxide nanoparticles analyzed by direct injection ICP-MS: influence of particle size, agglomeration state and sample matrix

Sylvie Motellier, Arnaud Guiot, Samuel Legros and Brice Fiorentino

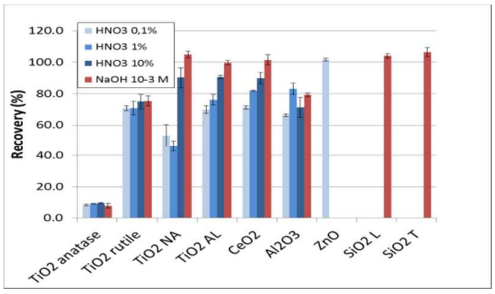

Metal oxide nanoparticles were analyzed by ICP-MS with direct injection and their recoveries were determined in different media.

JAAS

RSCPublishing

ARTICLE

Elemental recoveries for metal oxide nanoparticles analysed by direct injection ICP-MS: influence of particle size, agglomeration state and sample matrix

Sylvie Motellier[a*], Arnaud Guiot[a], Samuel Legros[b] and Brice Fiorentino[a]

Cite this: DOI: 10.1039/xoxxoooooox

Received ooth January 2012,
Accepted ooth January 2012

DOI: 10.1039/xoxxoooooox

www.rsc.org/

The direct analysis of metal-oxide nanoparticles (NPs) in suspension by inductively coupled plasma-mass spectrometry (ICP-MS) has been investigated. The roles of the chemical nature, size, crystalline form and agglomeration state of the particles on the recovery rate -compared with dissolved samples- have been investigated. Various sample matrices have been tested with the aim to optimize the decomposition process of the particles in the plasma, which governs the quality of the ICP-MS analytical results. It was found that, for SiO_2 and ZnO, full recovery was readily obtained in 10^{-3} mol L^{-1} NaOH or 0.1 % HNO_3, respectively. In the case of more stable oxides like TiO_2 or CeO_2, a positive correlation of the recovery with the concentration of the HNO_3 concentration in the matrix could be observed, although only NaOH could lead to identical sensitivities for NPs and ionic solutes. Al_2O_3 could not be satisfactorily analysed (80 % recovery at the most). Size and agglomeration state characterization of the selected particles was performed by scanning electron microscopy and dynamic light scattering. The effect of agglomeration state was found to be of minor influence but the size of the primary particle, as well as its crystalline phase play an important role on the analytical recovery.

Introduction

The rapid development of nanoparticles (NPs)-containing products in a wide variety of applications raises questions about their life cycle and fate, with particular concern for possible human and environmental exposures. In the context of assessing potential health and environmental risks, the detection, identification, and quantification of these specific particles represent a new challenge for analysts. Inductively coupled plasma-mass spectrometry (ICP-MS) is one of the preferred techniques for elemental analysis because of its high sensitivity and its multi-element capability. Traditionally, solids or slurries undergo digestion steps prior to their introduction into the analytical device. This treatment is intended to assure homogenization by decomposition of the analytes in a matrix that is compatible with the analytical method. However, it suffers from several drawbacks such as incomplete dissolution for a number of minerals and refractory compounds, possible losses of volatile elements, contamination problems and potential hazard due to the use of concentrated acids or bases, and time consumption. The pretreatment can be somewhat improved in efficiency and shortened by application of microwave-assisted digestion procedures [1]. In the case of refractory titania (TiO_2) however, and even with such boosted conditions, the best decomposition conditions require the addition of concentrated sulfuric acid that creates severe interferences with ^{48}Ti (abundance 74 %) or the use of concentrated HF and/or HCl that will deteriorate the quartz / glass sample introduction system of the ICP-MS [2, 3]. Furthermore, any type of digestion procedure will induce loss of information on the size, size distribution, and morphology of the initial colloïdal sample.

In order to perform complete characterization of the NPs, new analytical tools have been developed or adapted [4]. For instance, field flow fractionation (FFF), initially devoted to the hydrodynamic size-fractionation of macromolecules and sub-micro- to microparticles, has been successfully applied to the characterization of NPs size distribution [5-8]. It has the great advantage of being able to separate particles within a very large size range (from 1 nm to a few µm). Detection of the particles is generally performed by light scattering, UV or fluorescence. In the case of metal-containing particles, FFF

can be coupled with ICP-MS for improved chemical identification and quantification. In this particular case of hyphenated techniques, the sample is introduced directly into the ICP nebulization chamber and further into the plasma as a diluted suspension coming from the FFF outlet with no digestion pre-treatment.

Considering quantification purposes, the question that arises then is that of the recovery rate compared with the injection of dissolved samples. This concern has been extensively addressed in the case of slurry nebulization [9, 10] since the 1980s. This mode of direct injection of solid particle-containing suspensions into an ICP was initially proposed as an alternative to tedious sample treatments for the analysis of ceramics [11, 12] and geological samples [13-15]. More recently, the method has been applied to the quantification of nanoparticles in suspensions [7, 16]. Calibration using aqueous reference standards can be proposed as a very simple and attractive way of getting quantitative information. However, two points are of major importance in the control of the reliability of analytical calibration functions: i) sample introduction and nebulization system and ii) plasma-induced sample decomposition, atomization and ionization. During these two steps, efficiencies should be identical whether suspensions or aqueous solutions are analyzed.

Sample uptake efficiency and representativeness depends on parameters such as homogeneity and stability of the suspension [11]. Nebulization efficiency depends on density and size distribution of the particles; large particles with a high density are more susceptible to settle down in the spray chamber, which would lead to segregation in the sample transfer into the plasma. Halicz and Brenner [13] tested a number of geological materials ground at grain sizes below 2 µm prior to their introduction as slurries in the ICP. They did not observe material deposition in the sample introduction system, showing that nebulization did occur in a satisfactory manner for these small particles. These findings were reinforced by Ebdon et al. [17] who propose a maximum particle size of 3 µm for difficult samples like refractory minerals.

Still, even within these recommendations, satisfactory calibrations could not always be reached. Limitations can then be assigned to the textural, mineralogical, and chemical composition of the materials. For instance, dissociation of refractory particles can hinder the sample decomposition process in the plasma. In the experiments reported by Halicz and Brenner [13], it should be noted that the internal standard (dissolved Sc) did compensate for effects of slurry solid content (typically due to viscosity when solid content exceeds 0.5 %) but not for matrix and grain size interferences (observed through deviations in the correlation coefficients of the calibration curves of slurries compared with those of dissolved analytes). Brenner and Zander [18] hypothesize that these interferences effects are due to sample chemistry, mineralogy and particle size, which prevents compensation with aqueous internal standard that will obviously not behave as solid particles. Application of empirical correction factors can then be considered to compensate for lower intensity response of particles compared with aqueous analytes [14].

In the case of nanosuspensions, with a grain size far below this 2 – 3 µm threshold value, it is usually supposed that recovery rates should be 100 % whatever the particles, and a simple calibration procedure using aqueous dissolved certified standards for ICP-MS can be performed. This assumption has for instance been used in the analysis of nanoparticles released from exterior façade paints after runoff episodes [19]. However, in early laboratory experiments performed with silver and titania nanoparticles, we have experienced a severe discrepancy between the expected concentration and that obtained based on a simple aqueous calibration. Similar problems were reported by Fernandez-Ruiz et al. [20] in the analysis of Ru and Se in carbon nanoparticles. With their initial ICP-MS conditions, the recoveries obtained were only between 60 % and 80 %. An increase in RF power and a decrease in the nebulizer gas flow did increase the recovery values. Conversely, larger particles in the µm range seem to respond differently: in the case of clay particles, no improvement of the elemental recoveries could be obtained by increasing the Rf power [13, 15]. These observations show that at least one of the four processes involved as the sample aerosol droplet passes through the plasma (i.e. solvent evaporation from the sample matrix, vaporization of the matrix, atomization of the vaporized sample, and ionization of the analyte atoms) is not complete even though the particles are in the nano-size range.

The present study investigates the potentially peculiar behaviour of metal oxide nanoparticles (including some refractory materials) when directly injected as suspensions in an ICP-MS. The roles of chemical nature, crystallinity, size of the primary particle, and state of agglomeration have tentatively been pointed out with the intent to find satisfactory conditions for direct nano-suspensions analysis and keys for optimized detection conditions in FFF/ICP-MS hyphenated techniques.

Experimental

Sample preparation

Ultrapure water (Milli-Q, Millipore, Billerica, USA) was used throughout the experimental work.

For calibration purposes, nanoparticle suspensions were prepared by dispersion of nanopowders or dilution of commercial standard suspensions in either dilute HNO_3 (Suprapur quality, 65 wt. %, Merck, Darmstadt, Germany) or NaOH (Suprapur quality, monohydrate, Merck, Darmstadt, Germany). TiO_2 powders of anatase (< 25 nm) or rutile (< 100 nm) crystalline phases were from Aldrich (St Louis, USA). The commercial standard suspensions used in this study were TiO_2 NA (5 - 30 nm, anatase, 15 wt. % in water, Nanostructured and Amorphous Materials Inc., Houston, USA), TiO_2 AL (< 150 nm, mixture of rutile and anatase, 33 - 37 wt. % in water, Aldrich, St Louis, USA), CeO_2 (< 25 nm, 10 wt. % in water, Aldrich, St Louis, USA), Al_2O_3 (< 50 nm, 20 wt. % in water, Aldrich, St Louis, USA), ZnO (20 nm, Evonik, 35 wt. % in water, Essen, Germany), SiO_2 L (Ludox AS40, 20 - 24 nm, 40 wt. % in water, Sigma-Aldrich, St Louis, USA), and SiO_2 T (20 nm, 20 wt. % in water, Tecnan, Los Arcos, Spain). The weight percent concentrations of the commercial standard suspensions were checked firstly by drying an aliquote to completeness at 105 °C, and

then by subsequent calcination at 1000 °C of the residual powder. This second step was intended to verify the possible occurrence of organic stabilizing agents (namely surfactants) in the commercial standards. TiO_2 AL was estimated to be composed of ca. 35 % rutile and 65 % anatase (X-ray diffraction assays).

Reference calibration curves were established with ICP ionic standard solutions of Ti, Ce, Al, Zn (Tracecert 1000 mg L^{-1} in HNO_3 2 %,Fluka, Buchs, Switzerland), and Si (Tracecert 1000 mg L^{-1} in NaOH 2 %,Fluka, Buchs, Switzerland). 1000 mg L^{-1} (metal basis) stock standard suspensions were prepared in ultrapure water by either dispersion of the appropriate amount of powder or by dilution of the commercial suspensions. The latter were sonicated for 1 min in an ultrasonic cleaner (Branson, Danbury, USA) before sampling. The standard suspensions were then prepared by dilution of the stock suspensions (after homogenization by sonication treatment for 1 min) in the desired matrix. The final concentration range was between 0.5 µg L^{-1} and 10 µg L^{-1} (metal basis). For convenience of comparison between ionic and colloidal standards, all concentrations were expressed as metal content, independently of the primary particle size and/or possible aggregation/agglomeration processes in suspensions.

For scanning electron microscopy (SEM) characterizations, 10 µl aliquotes of 100 mg L^{-1} (metal basis) standard suspensions were deposited on polycarbonate membrane filters of 0.4 µm pore size and dried at 50°C on a hot plate. To prevent sample charging and damage from electron beam, samples were sputter coated with a 10-nm platinum layer. For dynamic light scattering (DLS) experiments, the measurements were made in triplicate with suspensions concentrations in the range 50 mg L^{-1} to 100 mg L^{-1} (metal basis). Due to the polydispersity of some of the analyzed samples, particle size could not be expressed as z-average. In order to allow simple comparison between samples, the choice was made to express all DLS size distribution results on a number basis.

Instrumentation

A muffle furnace was used for high temperature treatment of the nanoparticles (LHT 02/16 LBR from Nabertherm, Aubervillier, France). Dynamic light scattering measurements were performed using a Zetasizer Nano ZS (Malvern Instruments Ltd, Worcs, UK). The results are expressed as number-based particle diameters. Scanning electron microscopy was performed with an ultra-high resolution SEM LEO 1530 (LEO Electron Microscopy Ltd, Cambridge, England). To optimize the quality of SEM images, the working distance of sample was set at 4 mm, with an accelerating voltage of 5 kV and a diaphragm of 30 µm. The ICP-MS analyses were performed with a 7700x (Agilent Technologies, Santa Clara, USA) device equipped with a glass low-flow concentric nebulizer (400 µl min^{-1}), a quartz, low-volume Scott-type double-pass spray chamber, and a quartz torch with 2.5 mm internal diameter injector, Ni-sampler and Ni-skimmer cones, and a collision cell (not used in this study). Other operating conditions are listed in Table 1. Both the NPs suspensions and the ionic solutions were introduced in the ICP using an automated sampler ASX-520 (Agilent Technologies, Santa Clara, USA) by pumping them through a capillary tubing with the help of a built-in peristaltic pump. Stability of the ICP-MS was checked by analyzing the same calibration samples with a three-hour delay. Since the solid content of the suspensions was far below 0.5 %, no particular precaution was taken regarding viscosity-induced deviations and the analyses were performed without internal standard.

Table 1 ICP-MS operating conditions

RF power (W)	1550
Plasma gas (Ar) flow rate (L min^{-1})	15
Carrier gas (Ar) flow rate (L min^{-1})	1.01
Sampling depth (mm)	10
Integration time / mass (s)	0.1 (or 1)*
Replicates	3 (or 20)*
Sweeps/replicate	100

* Standard (or improved) conditions. See § Analytical quality.

Results and discussion

Characterization of the NP suspensions

Scanning electron microscopy SEM pictures were taken in order to check the size and the morphology of the primary particles. Examples of SEM pictures are given in Figure 1. An estimated mean value of the primary particle diameter was obtained by selecting random particles ($30 < n < 50$) and measuring their size. The mean diameter and the standard deviation for each type of particle are given in Table 2. It is obvious that the populations are very different, particularly with regard to size distribution. As observed in the SEM pictures, TiO_2 anatase, TiO_2 rutile, and ZnO look quite homogeneous in distribution. The same homogeneity was found for TiO_2 NA, TiO_2 AL, and SiO_2 L. Conversely, Al_2O_3 and, to a lesser extent, SiO_2 T and CeO_2 show very large differences in particle size, with large clusters made of very small particles coexisting along with larger primary particles (Figure 1d). Particle shape is also different: the anatase crystalline phase of TiO_2 has a distorted octahedral structure whereas the rutile phase looks more like slender

.

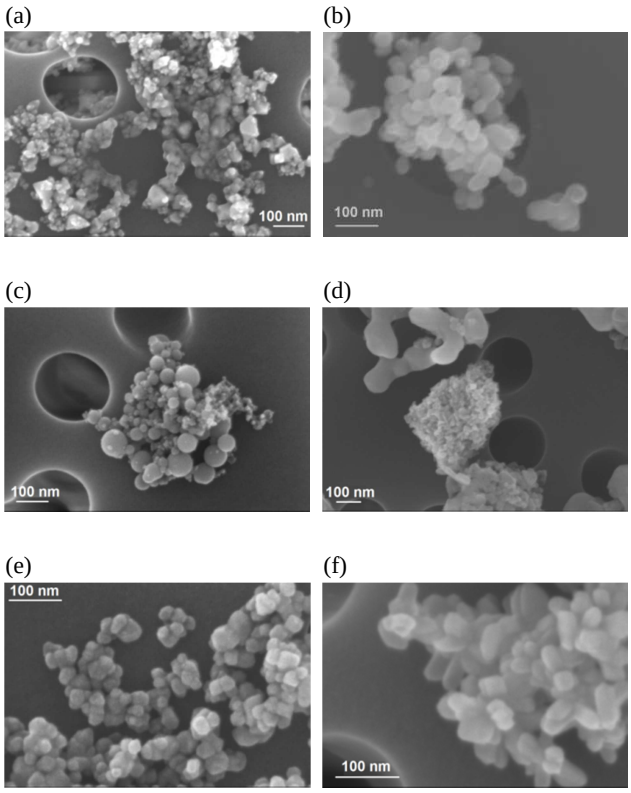

Fig. 1 SEM pictures of the nanoparticles. (a) CeO_2; (b) ZnO; (c) SiO_2 T; (d) Al_2O_3; (e) TiO_2 Anatase ; (f) TiO_2 rutile.

prismatic crystals [21]. Silica is mostly spherical while alumina and ZnO are irregular.

Dynamic light scattering The state of agglomeration of the colloids is a major concern when dealing with direct injection in ICP-MS. Indeed, a perfectly dispersed and steady suspension is a prerequisit to limit sedimentation within the sample vials and the introduction system. In order to evaluate the agglomeration behaviour of the selected NP in various possible injection matrices, DLS investigations were undertaken. The particles were diluted in either HNO_3 (0.1, 1, or 10 %) or NaOH (10^{-3} M). The latter matrix was chosen for SiO_2 analyses. In the most appropriate and widely used nitric medium, interferences will occur on all Si isotopes, leading to poor quantitative results. Besides, hydrated silica in colloidal form may encounter precipitation effects in acidic medium. Alkaline medium is thus preferred, although solubility is recovered only at high pH, which is not compatible with the silica-based sample introduction system. In order to limit degradation of the nebulizer and the spray chamber, a dilute NaOH solution was proposed as SiO_2 NP sample matrix. It should be noted that the concentrations used for DLS measurements are significantly higher than those used in ICP-MS experiments due to the lower sensitivity of the former method; the size values should only be considered as indicative of the particle behaviour in the different media.

Number-based diameters of the suspensions of interest are reported in Table 2. It is observed that the size recovered by DLS, even in water, is quite different from the one determined by SEM statistics treatments. Some particles, like TiO_2 anatase, show important agglomeration in aqueous medium: the mean diameter increases from 31.8 nm (primary particle, SEM estimation) to 205.7 nm (in water, DLS estimation). Others, like SiO_2, ZnO, TiO_2 NA and TiO_2 AL, seem to remain in a dispersed form. It is not easy to conclude in the case of Al_2O_3, mainly because of its extremely large size distribution. However, in pure water, Al_2O_3 particles do not seem to agglomerate. The alkaline medium does not promote agglomeration whatever the nature of the particles, witness the mean DLS sizes very close to those obtained by SEM. Nitric acid, on the contrary, has a drastic effect on the mean size of most particles (Figure 2). In dilute HNO_3 (0.1 %), no visible change can be seen with respect to water except for ZnO which readily dissolves. An increase in HNO_3 concentration induces a marked concomitant increase in particle diameter. The phenomenon is particularly visible for CeO_2, as well as for TiO_2 NA and TiO_2 AL. At such acidic pH, these particles are all positively charged and the agglomeration process is then possibly due to the increase in ionic strength that decreases the double layer thickness and favors inter-particle interactions.

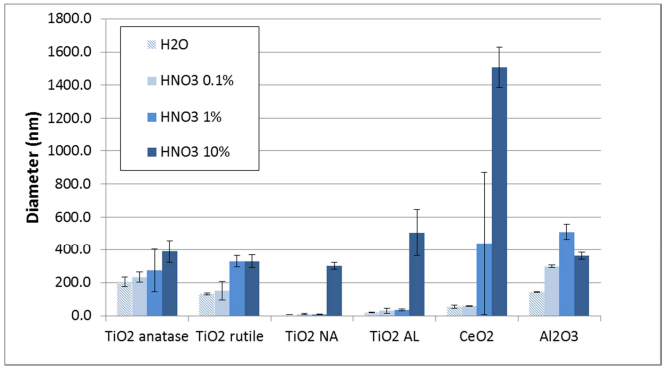

Fig. 2 Influence of the concentration of nitric acid on the size of the nanoparticles as measured by DLS (number-based).

Stability of suspensions The stability of the suspensions was evaluated by a second DLS measurement. The suspensions were left aside for three hours after preparation; they were re-analyzed without any further dispersing treatment (Table 2). In almost all instances, the mean diameter increases with time, which is consistent with an increase in the agglomeration state of the primary particles. It is noteworthy that the rate of agglomeration is not particularly speeded up by high acid concentrations. Rather, the formation of clusters occurs quickly when the particles are diluted in the acidic media, this step being acid-concentration dependent. Then, agglomeration seems to proceed at a rate depending on the nature of the particle.

Table 2 SEM and DLS (number-based) diameters of the NPs in various injection matrices.

3h : data obtained by DLS measurements 3h after the suspension preparation.

Diameter (nm) *(std dev)*	SEM	H_2O	NaOH 10^{-3} M	HNO_3 0.1%	HNO_3 1 %	HNO_3 10 %	HNO_3 0.1 %, 3h	HNO_3 1 %, 3h	HNO_3 10 %, 3h
TiO_2 anatase	31.8 *(7.6)*	205.7 *(30.6)*	48.7 *(1.6)*	233.9 *(32.1)*	276.3 *(129.2)*	390.6 *(66.6)*	173.5 *(8.1)*	622.0 *(8.8)*	504.1 *(61.4)*
TiO_2 rutile	78.9 *(8.4)*	132.3 *(6.4)*	80.7 *(4.1)*	150.4 *(56.1)*	329.8 *(35.0)*	330.0 *(39.3)*	552.4 *(29.3)*	854.5 *(9.2)*	640.0 *(20.6)*
TiO_2 NA	7.8 *(1.3)*	6.9 *(0.5)*	9.3 *(0.4)*	10.3 *(3.2)*	10.2 *(2.3)*	302.3 *(20.2)*	13.7 *(0.2)*	12.4 *(2.0)*	1064.6 *(141.9)*
TiO_2 AL	38.7 *(10.6)*	20.2 *(1.4)*	22.4 *(0.6)*	31.3 *(15.1)*	35.5 *(4.7)*	505.6 *(142.1)*	41.9 *(5.8)*	35.3 *(9.8)*	775.7 *(68.3)*
CeO_2	44.4 *(23.3)*	56.0 *(10.4)*	27.3 *(0.8)*	58.3 *(1.0)*	439.5 *(430.6)*	1507.7 *(120.2)*	62.2 *(8.1)*	1411.0 *(375.1)*	1084.0 *(44.2)*
Al_2O_3	246.9 *(167.4)*	142.7 *(2.5)*	182.0 *(3.4)*	299.3 *(7.7)*	511.1 *(47.2)*	364.6 *(20.4)*	482.1 *(6.5)*	687.4 *(21.0)*	554.2 *(18.3)*
ZnO	44.0 *(13.8)*	39.0 *(1.1)*	37.8 *(1.2)*						
SiO_2 L	31.1 *(4.0)*	12.9 *(0.8)*	13.4 *(0.2)*	13.6 *(0.1)*					
SiO_2 T	41.1 *(20.7)*	49.3 *(5.8)*	44.6 *(5.2)*	56.2 *(20.5)*					

ICP-MS measurements

In order to evaluate the performance of the analytical method with direct injection, calibration curves were plotted for all types of nanoparticles with the aim to find the sample matrix conditions that would lead to the best recovery compared with injection of ionic standards. The recovery was deduced from the slopes of the calibration curves linear fittings, by dividing the slope of the curve corresponding to the injection of the suspension standards by that of the ionic solution standards. The sets of suspensions were analyzed immediately after preparation. In order to verify that the threshold diameter of 2-3 µm found in previous studies for satisfactory introduction and nebulization [15, 17] would apply here, a second injection of the standard suspensions was made after waiting three hours. In the meantime, the suspension vials were left on the auto-sampler of the ICP-MS; they were not shaken prior to this second injection. In all cases, no significant difference between the first determination of the calibration curves and the second one could be observed. Recovery data given hereafter correspond to the mean value of both determinations.

Analytical quality Examples of calibration curves obtained with standard experimental conditions (see Table 1) are given in Figure 3a. Linearity is observed for ionic Ti standard solutions while, for direct injections of TiO_2 suspensions, linearity is rather poor, with large error bars on the data sets. This type of graph is significant of inhomogeneous samples: the particles injected into the torch via the nebulizer produce discrete events on the detector that drastically increase data dispersion.

JAAS RSCPublishing

ARTICLE

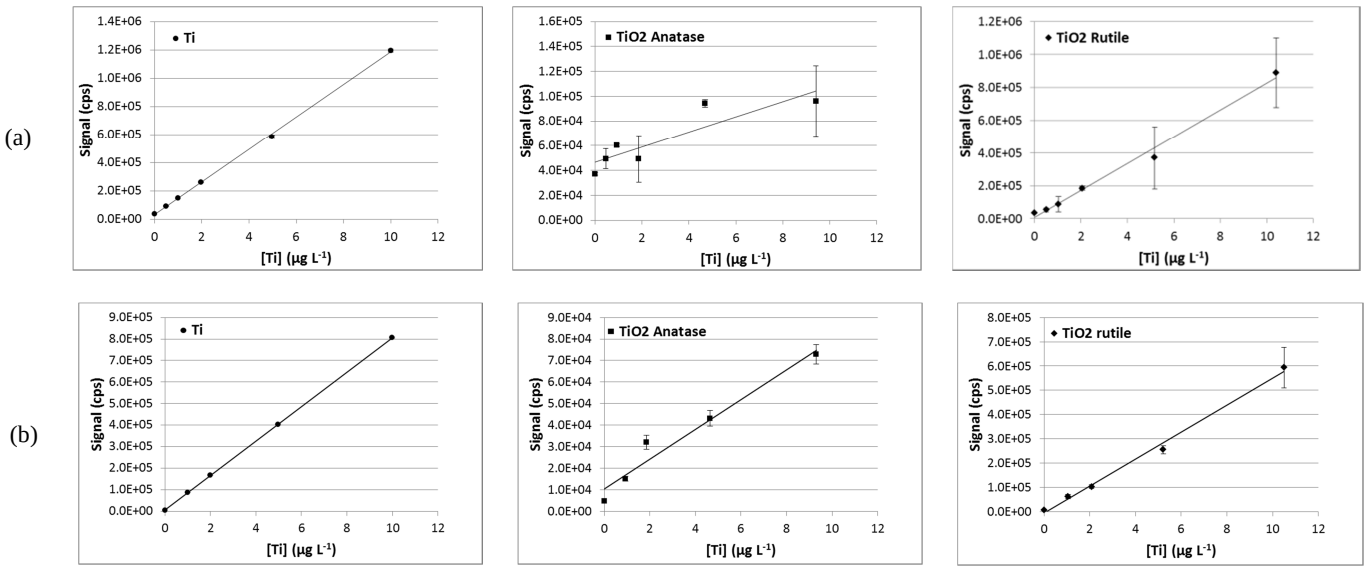

Fig. 3 Calibration curves of direct injections of Ti standard solutions and TiO_2 suspensions in HNO_3 0.1 %. (a) standard experimental conditions; (b) 20 replicates and 1s/mass integration time.

Obviously, the degradation in calibration linearity should be size- (and maybe even more size distribution-) dependent. Indeed, looking at the DLS sizes of TiO_2, it is observed that the anatase form of TiO_2, that shows the worst calibration curve correlation factor compared with the rutile form, agglomerates to larger clusters in HNO_3 0.1 % despite smaller primary particles.

As already observed [11], increasing the integration time and the number of replicates improved result quality, as demonstrated in Figure 3b. Because of a greater number of data acquired, dispersion is reduced and linearity is better in both anatase and rutile cases. This configuration of acquisition was chosen whenever needed, i.e. whenever the calibration curve correlation factor was below 0.99 with the usual operating conditions.

Effect of the suspension matrix on recovery The major objective of this study was to try to find experimental conditions for which the NPs suspensions would behave similarly to the ionic solutions when injected in the ICP-MS. Because of the general tendency of NPs to agglomerate in concentrated HNO_3, it was expected that dilute concentrations of this acid would give better recoveries. Three different concentrations (0.1, 1.0 and 10.0 %, in the usual range for ICP-MS analyses) were thus tested. NaOH, which was initially selected for SiO_2 NP analysis, was also tested with the other metal oxide NPs. An illustration of calibration curves obtained for CeO_2 NP with these experimental conditions is given in Figure 4. It is deduced from this graph that, contrary to the initial belief, the recovery increases with HNO_3 concentration despite the significant increase in particle diameter due to agglomeration (see Figure 2). However, it never reaches 100 % in this type of acidic matrix. Sodium hydroxide, on the contrary, does provide full recovery for this NP.

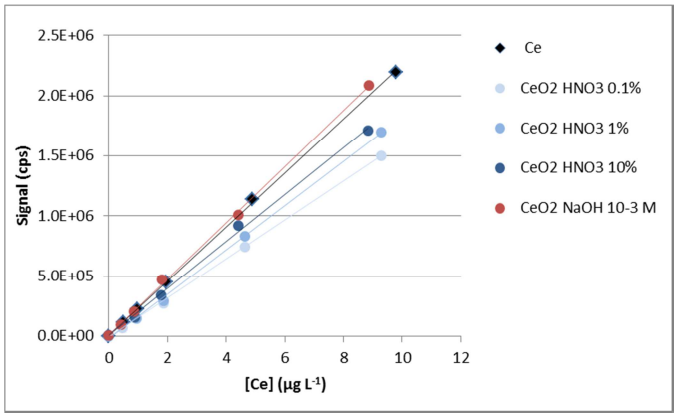

Fig. 4 Comparative calibration curves of CeO_2 NPs in different matrices directly injected in ICP-MS. The calibration curves established for NPs were normalized to the ionic Ce calibration curve.

Figure 5 gives an overview of the recoveries calculated for all the NPs investigated. The same conclusions can be drawn for almost all the NPs investigated: the injection recovery increases with HNO_3 concentration, but it always remains below that obtained in the alkaline matrix. The particular case of ZnO should be treated independently as this NP readily dissolves in acidic medium, even at the lowest tested HNO_3 concentration: its recovery is obviously 100% under such condition. SiO_2 NPs, although not in a dissolved state in NaOH matrix, also give full recovery when injected in this matrix.

TiO_2 NPs behave quite similarly to CeO_2 in acidic matrices. For almost all types of titania particles, an increase in ICP-MS recovery can be observed as the acid concentration increases. Likewise, the recovery is optimized in the alkaline matrix compared with the acidic media. The extent to which the recovery is modified by matrix changes depends on the type of TiO_2 particles. Namely, TiO_2 anatase and TiO_2 rutile are only little affected by the matrix of injection whereas TiO_2 NA and TiO_2 AL recoveries are highly matrix-dependent.

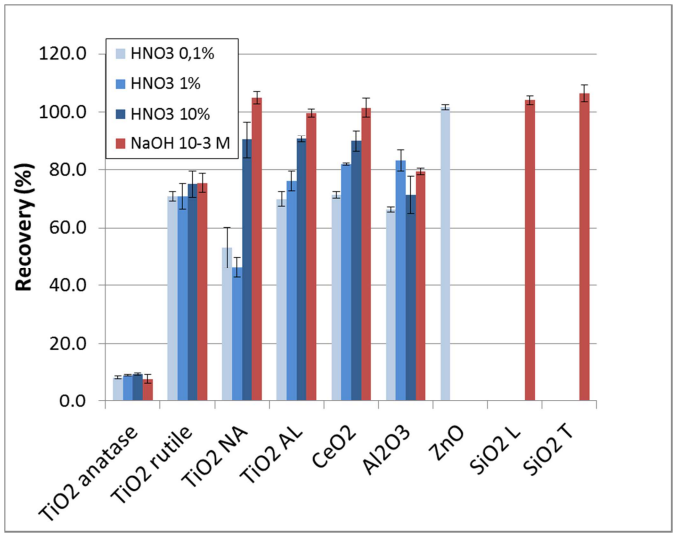

Fig 5 Effect of the injection matrix on the recovery of direct injection of nanoparticles.

Finally, in the case of alumina, there does not seem to be a clear influence of the matrix: in all cases (acid or alkaline conditions), the recovery data are scattered between 60 and 80 % with no specific tendency. This finding is consistent with those of Laird et al. [22] who did not find significant effect of the concentration of HNO_3 in the matrix solution on Al recovery in the analysis of clay minerals by slurry nebulization ICP-OES.

Nitric acid is the preferred matrix in the analysis of metal ions by ICP-MS since it is a strong acid with oxidizing properties that prevent them from precipitation and/or adsorption. However, the fate of metal oxide NPs differs from that of their ionic counterparts. The influence of the concentration of HNO_3 was tentatively assigned to the possible converse effects of two phenomena: the dissolution of the primary particles and the agglomeration processes, which are both favoured by high acid concentrations. The increase in recovery with acid concentration tends to show that the former be the prevailing effect. In high acid concentrations, particle-to-particle energy bonding involved within clusters is lower than intra-grain forces within a particle. This should promote the quick dissociation of agglomerates made of smaller -partially dissolved- particles in the plasma. Hence, in this instance, the state of agglomeration would be of minor influence on the analytical results.

Only NaOH alkaline matrix could lead to full ICP-MS recovery for the tested NPs. A possible explanation was proposed by Laird et al. [22] who found that elemental recoveries were significantly higher in 0.1 mol L^{-1} NaCl matrix than in 0.5 - 3 mol L^{-1} HNO_3 matrix. They suggest that the more complete dissociation-excitation of the particles promoted in the salt matrix may be caused by enhanced collisional dissociation due to the occurrence of high concentrations of Na^+ ions in the plasma. An additional explanation could lie in the difference in heat of vaporization, atomization and/or ionization energies of the matrix components that contribute to the loss of efficiency of heat transfer to the analytes.

The particular behaviour of alumina is possibly due to the highly refractive property of this material, coupled with the size dispersion of the primary particles. Indeed, the very large primary particles observed in Figure 1d may be more retained in the nebulization chamber than the smallest ones and those that will pass through are probably more difficult to decompose, vaporize, and atomize than smaller ones, or even than aggregates made of smaller primary particles; the residence time in the plasma may then be too short to enable maximum efficiency of these processes for these larger particles.

Effect of the nature and size of the primary particles on recovery

Whatever the observed results, the assumption of larger particles sedimentation in the sample vial (a supposedly phenomenon more important in the case of high HNO_3 concentrations) was rejected since the two consecutive injections (separated by a three-hour delay without re-homogenization) were not significantly different.

Looking at Figure 5, a great difference of behaviour can be observed between the four tested types of TiO_2 NPs. Three parameters can potentially play a role in this result: the state of aggregation/agglomeration in suspension, the size of the primary particles, and the nature of the crystalline phase

In the previous paragraph, agglomeration has been shown to be of limited effect on the recovery. Conversely, a comparison between TiO_2 anatase and TiO_2 NA, both made of pure anatase, indicates that the size of the primary particles plays a fundamental role: TiO_2 anatase particles (SEM diameter = 31.8 nm) is not decomposed/ionized in the plasma as efficiently as the smaller TiO_2 NA particles (SEM diameter = 7.8 nm). The same conclusion can be drawn from the data obtained with TiO_2 rutile and TiO_2 AL: TiO_2 rutile (SEM diameter = 78.9 nm) is decomposed/ionized less efficiently than the rutile fraction of TiO_2 AL (SEM diameter = 38.7 nm).

A comparison between the two samples obtained from dissolution of pure crystalline phases powders in pure water (TiO_2 anatase and TiO_2 rutile) shows that the anatase form stays below 10% recovery whereas the rutile form reaches 70%. In both cases, only little effect of the matrix can be observed. If only the size of the primary particles was to be considered, one would expect that the smallest anatase phase yield the highest recovery. Besides, in NaOH 10^{-3} M, the DLS size measurements are very close to those of SEM, showing that the particles are virtually not agglomerated in this matrix. This tends to show that the nature of the crystalline phase is a key factor in the direct introduction recovery rate in ICP-MS measurements. The important difference in efficiency between the two crystalline phases of TiO_2 NPs can be partly understood by the following considerations. At the nanoscale, it is more difficult to obtain good crystalline rutile NPs than anatase [23] and anatase becomes the more stable phase below 10 - 15 nm [24]. Hence, a highly crystalline and stable anatase phase NP like TiO_2 anatase will probably resist to the plasma decomposition effect better than a less crystalline and possibly less stable rutile phase NP like TiO_2 rutile. It has been reported that a decrease in pH would favor the anatase to rutile transformation in nanosuspensions of TiO_2 [25]. If rutile decomposes more readily in the plasma than anatase, as discussed above, this finding would be consistent with the increase of recovery observed with increasing acid concentration.

Conclusions

In the present study, some aspects of the particular behaviour of metal oxide nanoparticles analyzed by direct injection ICP-MS have been pointed out. Contrary to the general belief, a particle size in the nano range does not guarantee total plasma decomposition and perfect superposition of the calibration curve with that of the corresponding ionic standard. The most common 1% nitric acid matrix does not promote result quality, except for ZnO that readily dissolves in this medium. Although inducing agglomeration, a higher HNO_3 concentration improves the analytical results but the alkaline sodium hydroxide matrix presented the best results for all the NPs tested and did achieve 100 % recovery in the best case. While agglomeration state does not seem to play an important role in the recovery, primary particle size and crystalline form are of major influence. The analysis performs quite satisfactorily for NPs with size of the primary particle below 50 nm, except for TiO_2 anatase for which the size needs to be decreased around 10 nm. When the size of the primary particle is above 80 nm (TiO_2 rutile and Al_2O_3) the recovery decreases substantially. Hence, sensitivity should be carefully checked when dealing with quantitative analyses. In the case of hyphenated techniques like FFF/ICP-MS for which pretreatment of the suspension is not allowed, sensitivity optimization can be proposed by introduction of post-separation reagents in the effluent stream before entering the ICP.

Acknowledgements

The authors wish to thank Claude Chabrol and Sonia De Sousa Nobre for the XRD experiments for estimating the crystalline phase composition of TiO_2 AL. This work was supported by funds from the French Research National Agency in the frame of the EQUIPEX NANOID project.

Notes and references

[a] CEA, DRT/LITEN/DTNM/SEN/Laboratory for Nano characterization and Nano safety, 17 rue des martyrs, F-38054 GRENOBLE CEDEX

[b] CIRAD, UPR Recyclage et risque, Avenue Agropolis, F-34398 MONTPELLIER

1. F. E. Smith and E. A. Arsenault, *Talanta*, 1996, **43**, 1207-1268. DOI: 10.1016/0039-9140(96)01882-6.
2. M. D. A. Korn, A. C. Ferreira, A. C. S. Costa, J. A. Nobrega and C. R. Silva, *Microchem J.*, 2002, **71**, 41-48. DOI: 10.1016/s0026-265x(01)00119-9.
3. A. H. El-Sheikh and J. A. Sweileh, *Talanta*, 2007, **71**, 1867-1872. DOI: 10.1016/j.talanta.2006.08.029.
4. M. Hassellov, J. W. Readman, J. F. Ranville and K. Tiede, *Ecotoxicology*, 2008, **17**, 344-361. DOI: 10.1007/s10646-008-0225-x.
5. F. von der Kammer, P. L. Ferguson, P. A. Holden, A. Masion, K. R Rogers, S. J. Klaine, A. A. Koelmans, N. Horne and J. M. Unrine, *Environ. Toxicol. Chem.*, 2012, **31**, 32-49. DOI: 10.1002/etc.723.
6. L. Calzolai, D. Gilliland and F. Rossi, *Food Addit. Contam. Part A-Chem.*, 2012, **29**, 1183-1193. DOI: 10.1080/19440049.2012.689777.
7. P. Krystek, A. Ulrich, C. C. Garcia, S. Manohar and R. Ritsema, *J. Anal. At. Spectrom.*, 2011, **26**, 1701-1721. DOI: 10.1039/c1ja10071h.
8. S. Dubascoux, I. Le Hecho, M. Hassellov, F. Von der Kammer, M. P. Gautier and G. Lespes, *J. Anal. At. Spectrom.*, 2010, **25**, 613-623. DOI: 10.1039/b927500b.
9. P. Goodall, M. E. Foulkes and L. Ebdon, *Spectroc. Acta Pt. B-Atom. Spectr.*, 1993, **48**, 1563-1577. DOI: 10.1016/0584-8547(93)80143-i.
10. L. Ebdon, M. Foulkes and K. Sutton, *J. Anal. At. Spectrom.*, 1997, **12**, 213-229. DOI: 10.1039/a604914a.
11. J. C. Farinas, R. Moreno and J. M. Mermet, *J. Anal. At. Spectrom.*, 1994, **9**, 841-849. DOI: 10.1039/ja9940900841.
12. J. A. C. Broekaert, C. Lathen, R. Brandt, C. Pilger, D. Pollmann, F Tschopel and G. Tolg, *Fresenius J. Anal. Chem.*, 1994, **349**, 20-25. DOI: 10.1007/bf00323218.
13. L. Halicz and I. B. Brenner, *Spectroc. Acta Pt. B-Atom. Spectr.*, 1987, **42**, 207-217. DOI: 10.1016/0584-8547(87)80062-9.
14. L. Halicz, I. B. Brenner and O. Yoffe, *J. Anal. At. Spectrom.*, 1993, **8**, 475-480. DOI: 10.1039/ja9930800475.
15. D. A. Laird, R. H. Dowdy and R. C. Munter, *Soil Sci. Soc. Am. J.*, 1991, **55**, 274-278.
16. R. Allabashi, W. Stach, A. de la Escosura-Muniz, L. Liste-Calleja and A. Merkoci, *J. Nanopart. Res.*, 2009, **11**, 2003-2011. DOI: 10.1007/s11051-008-9561-2.
17. L. Ebdon, M. E. Foulkes and S. Hill, *J. Anal. At. Spectrom.*, 1990, **5**, 67-73. DOI: 10.1039/ja9900500067.
18. I. B. Brenner and A. Zander, *Fresenius J. Anal. Chem.*, 1996, **355**, 559-570.
19. R. Kaegi, A. Ulrich, B. Sinnet, R. Vonbank, A. Wichser, S. Zuleeg, H. Simmler, S. Brunner, H. Vonmont, M. Burkhardt and M. Boller, *Environ. Pollut.*, 2008, **156**, 233-239. DOI: 10.1016/j.envpol.2008.08.004.
20. R. Fernandez-Ruiz, P. Ocon and M. Montiel, *J. Anal. At. Spectrom.*, 2009, **24**, 785-791. DOI: 10.1039/b819922a.
21. N. S. Allen, M. Edge, T. Corrales, A. Childs, C. M. Liauw, F. Catalina, C. Peinado, A. Minihan and D. Aldcroft, *Polym. Degrad. Stabil.*, 1998, **61**, 183-199. DOI: 10.1016/s0141-3910(97)00114-6.

22. D. A. Laird, R. H. Dowdy and R. C. Munter, *J. Anal. At. Spectrom.*, 1990, **5**, 515-518. DOI: 10.1039/ja9900500515.
23. Y. Ju-Nam and J. R. Lead, *Sci. Total Environ.*, 2008, **400**, 396-414. DOI: 10.1016/j.scitotenv.2008.06.042.
24. H. Z. Zhang and J. F. Banfield, *J. Phys. Chem. B*, 2000, **104**, 3481-3487. DOI: 10.1021/jp000499j.
25. Y. Hu, H. L. Tsai and C. L. Huang, *Mater. Sci. Eng. A-Struct. Mater. Prop. Microstruct. Process.*, 2003, **344**, 209-214. DOI: 10.1016/s0921-5093(02)00408-2.
26. W. Thongsuwan, T. Kumpika and P. Singjai, *Curr. Appl. Phys.*, 2011, **11**, 1237-1242. DOI: 10.1016/j.cap.2011.03.002.
27. S. K. Esthappan, S. K. Kuttappan and R. Joseph, *Polym. Degrad. Stabil.*, 2012, **97**, 615-620. DOI: 10.1016/j.polymdegradstab.2012.01.006.